Computational Mechanics 31 (2003) 496–504 © Springer-Verlag 2003
DOI 10.1007/s00466-003-0457-9

Optimization of airbag inflation parameters for the minimization of out of position occupant injury

P.-O. Marklund, L. Nilsson

Abstract In this paper optimization techniques together with coupled fluid-structure analysis are used to provide a better understanding of the interaction between the airbag inflation process and an Out Of Position occupant. We provide a concept for, and exemplify how these techniques can be applied to optimize the airbag inflator characteristics in order to minimize occupant injury. For a simplified, but realistic, problem we show that the head acceleration can be reduced by approximately 65% by optimizing the inlet characteristics.

Keywords Airbag inflation, Optimization, Response surface

1
Introduction

The National Highway Traffic Safety Administration, NHTSA (2001), in the United States estimates that 7600 people have been saved by airbag systems between 1990 and 2001. But at least 119 children and 76 adults have also been killed by airbags during the same period of time. The majority of these fatalities occurs when the occupant is situated too close to the airbag as it inflates, commonly termed Out Of Position (OOP) occupants. These accidents primarily occur at low impact speeds.

Increasing demands from authorities and customers make the OOP problem of high priority for the automotive industry. Many steps have been taken, e.g. many car models now have depowered airbag inflator modules installed. Depowered inflators basically consist of two smaller charges instead of one large and depending on the severity of the crash, only one or both of these charges are ignited.

Received: 11 October 2002 / Accepted: 21 May 2003

P.-O. Marklund (✉)
Engineering Research, Garnisonen,
Brigadgatan 16, SE-58131 Linköping, Sweden
E-mail: per-olof.marklund@erab.se.

L. Nilsson
Division of Solid Mechanics, Linköping University, Sweden

This work is funded by Autoliv Research and the Swedish Agency for Innovation Systems (VINNOVA). The authors would like to thank Dr. Bengt Pipkorn, Dr. Yngve Håland and Mr. Claes-Fredrik Lindh at Autoliv Research for help on airbag issues, Dr. John Hallquist for giving us the possibility to use LS-DYNA and Dr. Nielen Stander for helpful discussions on optimization techniques.

In this study we will provide an example how Finite Element (FE) simulation techniques together with optimization procedures can be used to optimize the inflator characteristics in order to minimize the occupant injury. We will start with a neutral design, and let the optimization procedure determine the final design, i.e. independent of how an input mass flow curve looks today or what is possible to achieve with today's technology. The model which is used is simplified compared to the model that would be needed for commercial product, but it still includes many of the difficulties, such as folding and OOP resistance.

To simulate the airbag inflation process a coupled fluid-structure approach will be used. This procedure has a great advantage compared to the control volume concept, which is currently used by almost all car manufacturers. It can predict pressure variations both in time and in space, making it ideal to simulate impact with OOP occupants. The disadvantage with the method is that the cpu-time required is substantially larger.

Coupled fluid-structure analysis has only been used recently for airbag inflation analysis and the publication list available is relatively short. The reader should consult the following references for more insight: Marklund and Nilsson (2002a,b), Mestreau and Löhner (1996), Zhu et al. (1999), Ullrich et al. (2000) and Kamiji and Kawamura (2001).

2
Fluid-structure coupling

The fluid-structure coupling algorithm used in the present study is based on Olovsson (2000) and it is currently available in the finite element code LS-DYNA.

In this algorithm the Lagrangian structure can move freely in a structured Eulerian (or Arbitrary Lagrangian Eulerian) finite element mesh, and forces are transferred between the fluid and the structure through a penalty contact algorithm.

Assuming frictionless contact the following expression for the coupling force $\mathbf{F}_{\mathbf{coup}}$ can be derived

$$\boldsymbol{F}_{\text{coup}} = [k\boldsymbol{d}_{\text{coup}} \cdot \hat{\mathbf{n}}]\hat{\mathbf{n}} \ , \tag{1}$$

where $\boldsymbol{d}_{\text{coup}}$ is the penetration vector and $\hat{\boldsymbol{n}}$ is the unit normal of the structural element, see Fig. 1. The penalty stiffness k is set to a few percent of the critical stiffness, i.e. the stiffness which will cause instability of the mass and spring system, see e.g. Hughes (1987).

$$k = \alpha \frac{m^*}{\Delta t^2} \tag{2}$$

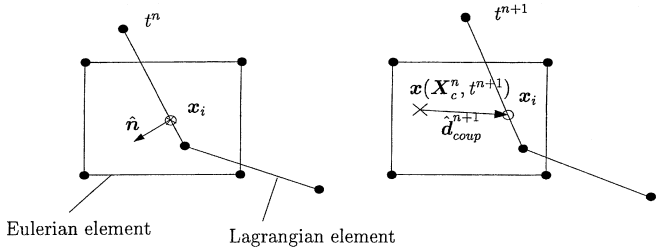

Fig. 1. Displacement tracking

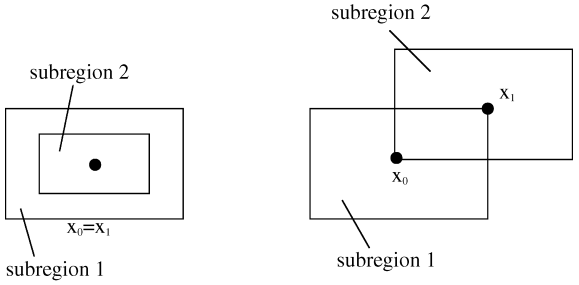

Fig. 2. Panning and zooming in SRSM

$$m^* = \min[m_l, m_e] \tag{3}$$

α is a scaling constant, usually $\alpha \approx 0.01 - 0.1$, m_l is the mass associated with the Lagrangian coupling point and m_e is the interpolated mass associated with the corresponding point in the Eulerian element.

The coupling forces are then transferred to the nodes of the Lagrangian and Eulerian elements, respectively

$$\boldsymbol{F}_{L,j}^{n+1} = -N_{L,j}\boldsymbol{F}_{\text{coup}} \tag{4}$$

$$\boldsymbol{F}_{E,j}^{n+1} = N_{E,j}\boldsymbol{F}_{\text{coup}} \ , \tag{5}$$

N_L are the bilinear shape functions for the Lagrangian elements and N_E the trilinear shape functions for the Eulerian elements. Finally, the internal Lagrangian and Eulerian forces are assembled into the corresponding global vectors.

When applying this algorithm to airbag inflation problems one must keep in mind that it can only be used for airbags without fabric porosity. This is caused by the penalty contact algorithm that penalizes all penetrations, making it difficult to control the leakage through the fabric.

Fabric porosity can be neglected if the fabric weave is covered with a thin liner, e.g. silicon.

The interested reader should consult Olovsson (2000), and Marklund and Nilsson (2002a,b) for more details.

3
Response surface optimization

As airbag inflation simulations are highly non-linear, care has to be taken when choosing the optimization method. Optimization using the Response Surface Method (RSM) has been shown to be both stable and efficient when the number of design variables are kept reasonably low, see e.g. Roux et al. (1998), Marklund and Nilsson (2001) and Redhe et al. (2002b). The method tends to succeed where local gradient methods fail, which primarily is where noisy responses are present.

Using response surface optimization methods, we do not start at a single design point, but rather over an area in the design space. Over this area we want to fit surfaces for the cost and constraints in the design space. These surfaces can be written as:

$$g_i = \boldsymbol{X}_i\beta_i \quad i = 1, 2, ..., p \ \text{ No summation} \tag{6}$$

where p is the total number of surfaces and $\boldsymbol{X}$ contains the polynomial terms of the surface. The coefficients β are found through the following steps:

1. Find a set of starting points using the D-optimality criterion, see Myers and Mongomery (1995), i.e. from a user given number of design points find the values which
$$\max\left[\det(\boldsymbol{X}^{\mathrm{T}}\boldsymbol{X})\right] \ . \tag{7}$$
2. Compute the values of cost and constraints at the design points chosen in the last step.
3. Fit cost and constraints surfaces in the design space using a least square approximation.
4. Use a gradient-based method to find an optimum in the reduced problem.
5. The optimum is found if certain convergence criteria are met. If not, increase the order of the surfaces and/or reduce the design region of interest and go back to step one.

In order to check the convergence, the errors of the response surfaces must be examined. This is often done by using check points that are not included in the surface fitting. The cost and constraint values at these check points are compared to the corresponding approximated values. If the errors are small and the optimum is found within the region of interest, the optimization problem has converged.

The design region of interest is often initially chosen as the whole design range and in each iteration the region of interest is decreased successively, see Roux et al. (1998) and Stander (2001). This procedure is often denoted as the Successive Response Surface Method (SRSM). Basically, if the optimum design point in one iteration is found on the inside of the region of interest, the size of the subregion is centered around that point and decreased. If the optimum point is found on the boundary of the region of interest, the subregion is moved, see Fig. 2.

For linear response surfaces with n design variables, the surface expression takes the form

$$g = \beta_0 + \beta_1 x_1 + \cdots + \beta_n x_n \ . \tag{8}$$

To determine the unknown constants β_0 to β_n at least $n+1$ design points are needed. For quadratic response surfaces this number rises to $(n+1)(n+2)/2$. It is not recommended to use the minimum number of design points as the error of the surface fit will be too high. A general recommendation for crashworthiness problems is that at least 50% more than the minimum number should be used, see Redhe et al. (2002a).

4
Airbag inflation optimization

There are many factors affecting the behavior of an airbag inflation. Factors such as

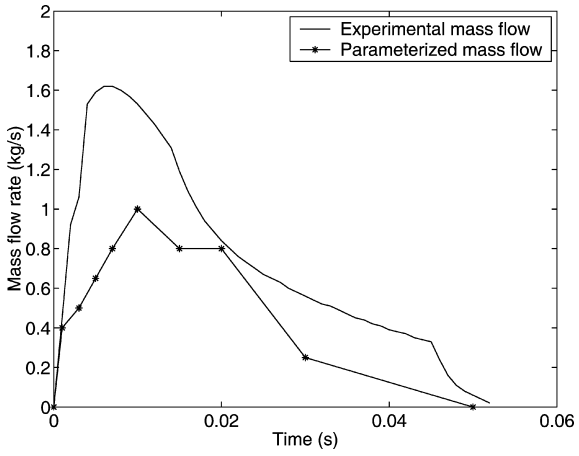

Fig. 3. Parametric mass flow shown together with an experimental mass flow curve

- input mass flow,
- gas characteristics,
- folding,
- containment,
- fabric characteristics,
- vent holes (size and position) and
- bag volume

are all important during the deployment process.

The factor which will be considered in this optimization is the input mass flow rate. The mass flow curve is parameterized using 8 design variables, q_1 to q_8. These points are located at fixed values of time, after 1, 3, 5, 7, 10, 15, 20 and 30 ms. The chosen values of time are purposely concentrated to the early time states, since the OOP occupant is primarily affected during this time. Between these points the mass flow curve is interpolated linearly, see Fig. 3.

One additional factor has also been considered outside the optimization, i.e. the position of the venting holes. This factor has not been included in the optimization, for reasons which will be explained later. The reason why only the position of the venting holes, and not the size is considered, is that airbags are primarily designed for in position crashes, and the venting holes are sized thereafter.

4.1 Airbag model

The FE simulation model mainly consists of three parts:

- The folded airbag, which is modeled using membrane shell elements with isotropic elastic properties, i.e. Young's modulus, $E = 500$ MPa and Poisson ratio $\nu = 0.3$. The folded configuration is achieved by 12 folding operations carried out in the preprocessor LS-INGRID. This is shown in Figs. 4 and 5.
- The fluid mesh, which is an Arbitrary Lagrangian Eulerian (ALE) mesh. This means that the mesh can move independently of the material flow, see e.g. Belytschko et al. (2000). Using this technique, we can expand the fluid mesh as the inflation process progresses, and therefore achieve a better accuracy at the early stages of the inflation process without using an unrealistic number of elements. Currently, the mesh can only be expanded in the direction of the flow. Otherwise the inlet conditions would be compromised as the inlet area would change during expansion. The inlet conditions are further described in Sect. 2. The fluid is modeled with inviscid compressible properties.
- The head form, which is a representative model of a human head regarding mass and inertia properties, but with a spherical shape. This part is modeled as a rigid body.

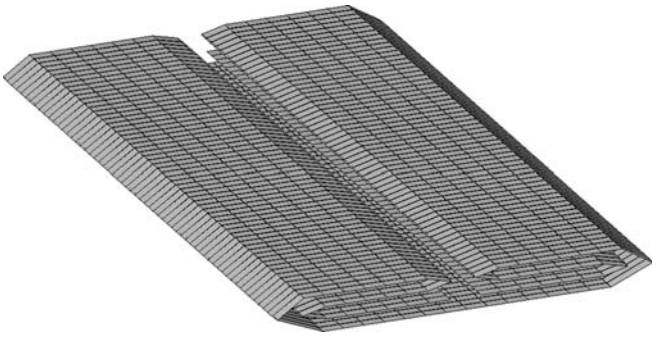

Fig. 4. Folding in first direction. The fold thickness is increased for visualization purpose

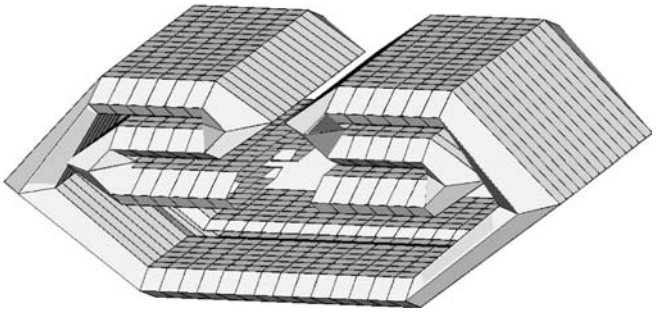

Fig. 5. Folding in second direction. The fold thickness is increased for visualization purpose

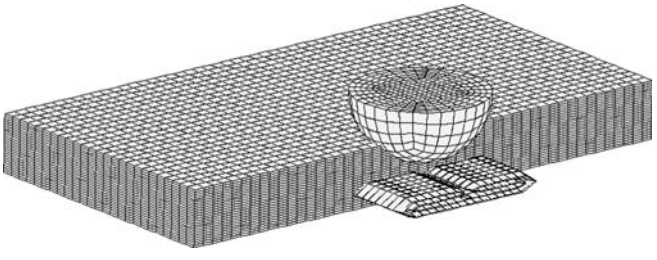

Fig. 6. Finite element model setup

These parts are shown in Fig. 6. In this figure, half of the fluid mesh is blanked out for visualization purpose. Figure 7 shows the usage of the ALE concept for expanding the fluid mesh.

The complete model consists of approximately 60 000 fluid elements and 7200 shell elements. It takes about 12 h of cpu-time on one 1.4 GHz PC processor running Linux to reach the response time of 40 ms.

4.2 Airbag inlet conditions

The thermomechanical data of a pyrotechnic gas inflator is supplied in the form of a mass flow curve and a tempera-

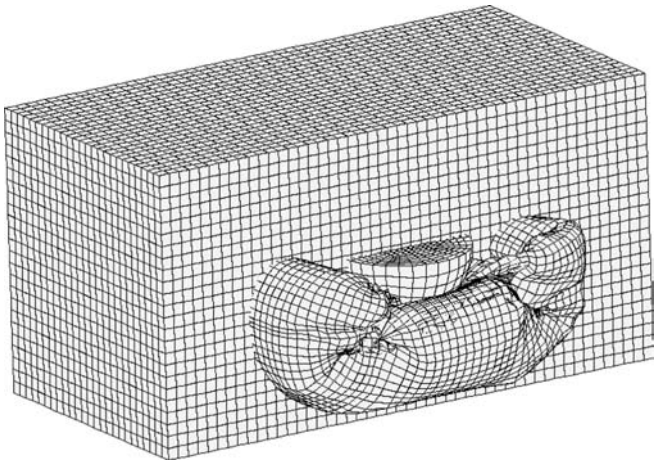

Fig. 7. Expanding fluid mesh

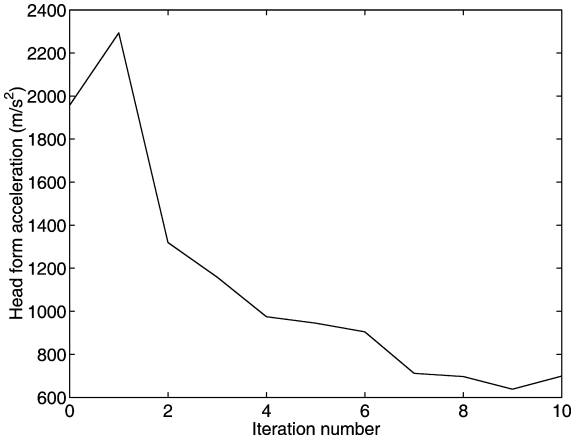

Fig. 8. Head form acceleration in each iteration

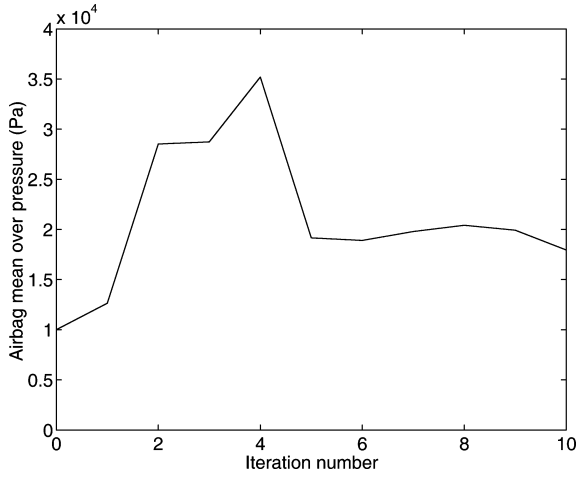

Fig. 9. Airbag mean pressure at 30 ms in each iteration

ture curve. The mass flow curves have traditionally been used together with a control volume simulation technique. The mass flow and temperature curves are found through tank tests, where the gas is inflated into a rigid tank.

When the Navier-Stokes equations are used for the fluid, more boundary conditions, in addition to the mass flow and temperature, are needed.

Table 1. Computed vs. predicted results in iteration 9 and 10

Iteration	Response	Computed	Predicted	Error (%)
9	Acceleration (m/s^2)	638.2	615.5	3.7
	Bag pressure (Pa)	$1.199 \cdot 10^5$	$1.2 \cdot 10^5$	0.08
10	Acceleration (m/s^2)	699.1	615.5	13.6
	Bag pressure (Pa)	$1.179 \cdot 10^5$	$1.2 \cdot 10^5$	1.75

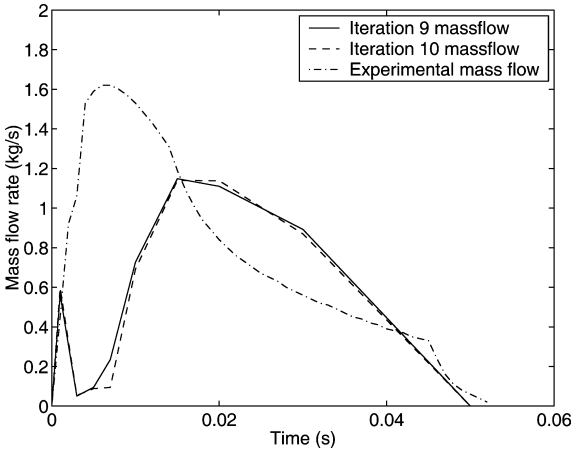

Fig. 10. Optimized mass flow curve

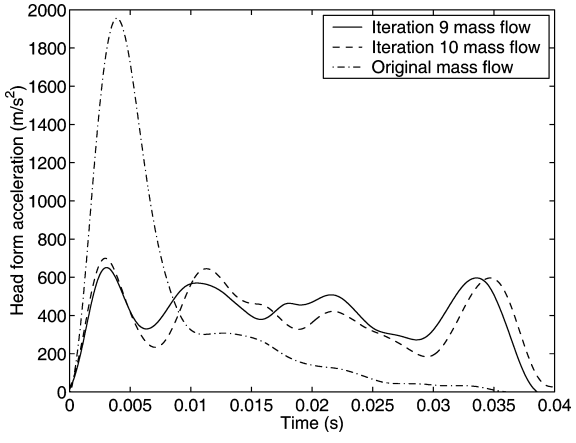

Fig. 11. Head form acceleration for the initial and the optimal design. The results are filtered using a 100 Hz low pass filter

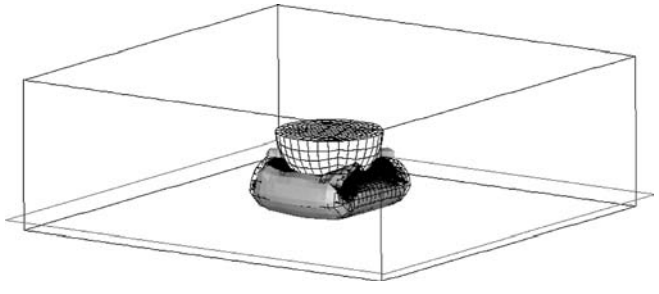

Fig. 12. Inflated configuration at t = 5 ms

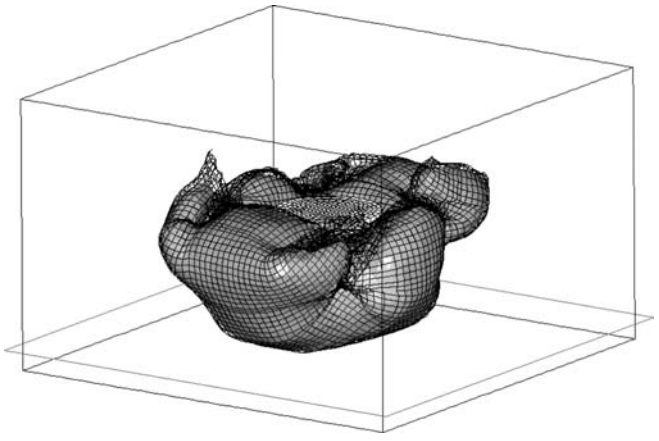

Fig. 13. Inflated configuration at t = 20 ms

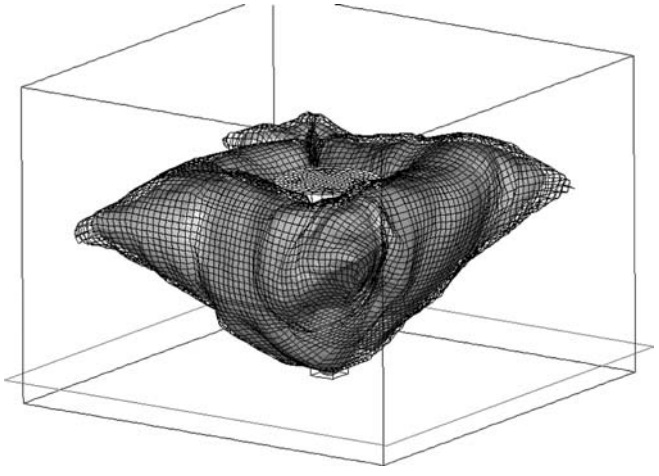

Fig. 14. Inflated configuration at t = 30 ms

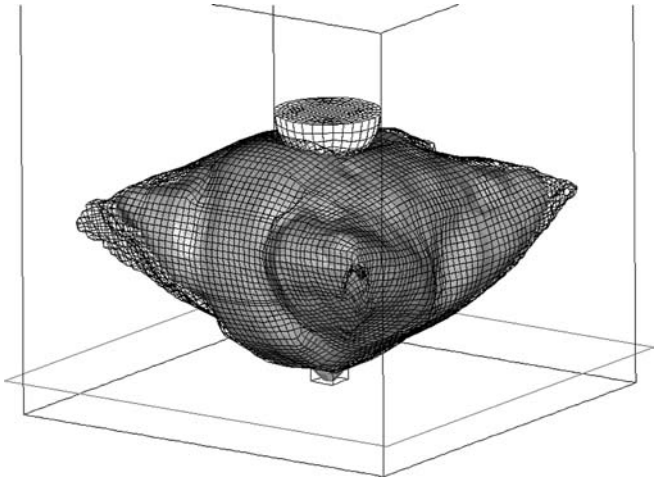

Fig. 15. Inflated configuration at t = 35 ms

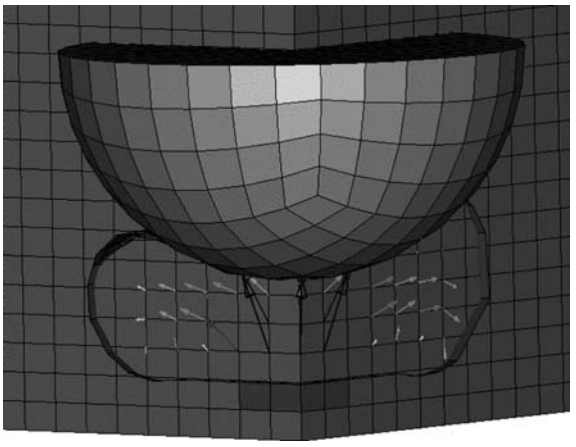

Fig. 16. Velocity profile at t = 5 ms. Dark arrows represent high velocity, light arrows represent low velocity

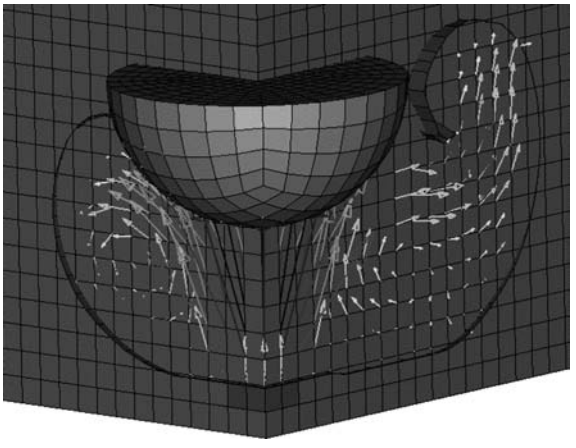

Fig. 17. Velocity profile at t = 20 ms. Dark arrows represent high velocity, light arrows represent low velocity

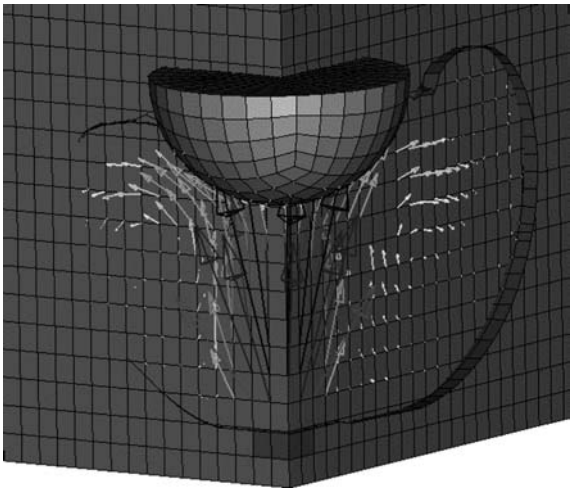

Fig. 18. Velocity profile at t = 30 ms. Dark arrows represent high velocity, light arrows represent low velocity

If the gas is assumed to follow the perfect gas law,

$$p = \rho RT \ , \tag{9}$$

where p is the pressure, ρ the density, R the gas constant and T the absolute temperature, two of the three variables above have to be given as inlet conditions. The mass flow, $\dot{m}$, is defined as

$$\dot{m} = \rho A v \ , \tag{10}$$

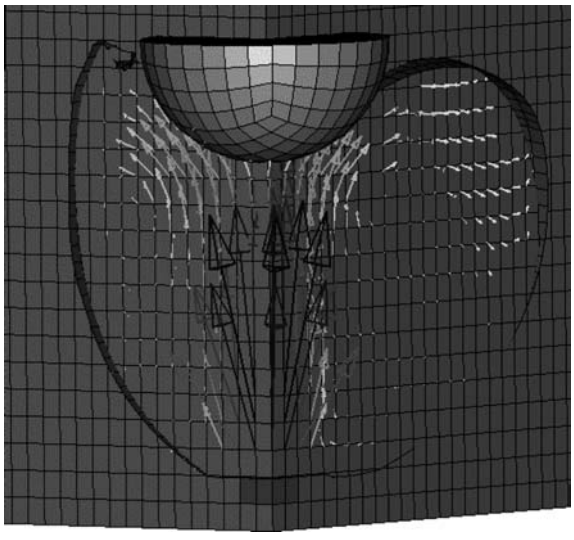

Fig. 19. Velocity profile at t = 35 ms. Dark arrows represent high velocity, light arrows represent low velocity

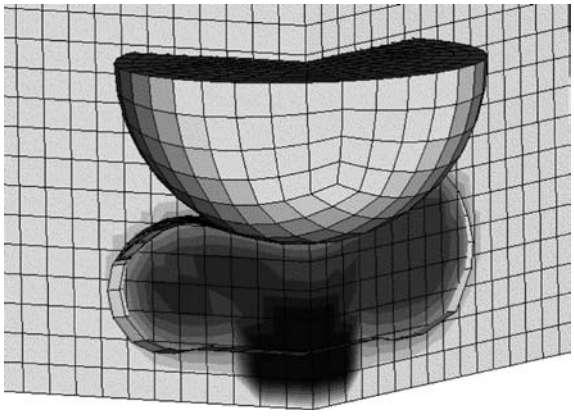

Fig. 20. Original bag: pressure at 5 ms. $p_{\max} = 3.06 \cdot 10^5$ Pa

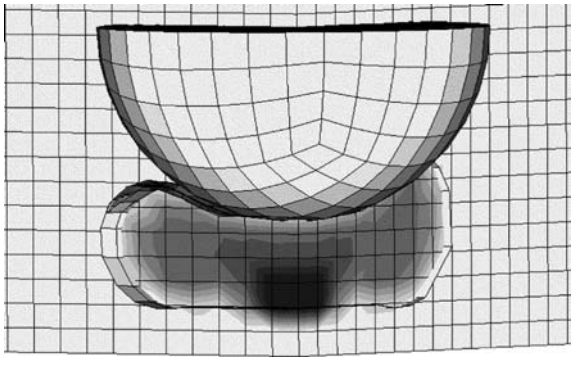

Fig. 21. Optimal bag: pressure at 5 ms. $p_{\max} = 2.14 \cdot 10^5$ Pa

where A is the inlet area and v the mean inlet velocity. Equations (9 and 10) contain three unknowns, p, ρ and v, but only two equations are available. If, at this point, no further information is available, assumptions are needed. There are mainly two alternatives.

1. Consider the inlet velocity to be sonic. This assumption is often, but not always, true until the airbag has reached the state where tensile stresses develops in the fabric and the pressure increases. If the ratio between the inflator pressure, p_i, and the pressure just inside the bag, p_{b1}, fulfills
$$\frac{p_i}{p_{b1}} \geq \left(\frac{\gamma+1}{2}\right)^{\frac{\gamma}{\gamma-1}} \tag{11}$$
there is sonic flow, see Anderson (1982). γ is the ratio between the specific heats at constant pressure and constant volume, $\gamma = c_p/c_v$. At the early stages of inflation this can be compromised by some resisting force, e.g. a human body very close to the inflation point. This may allow a high pressure zone to be built up locally and Eq. (7) is not fulfilled. This phenomenon was observed in Marklund and Nilsson (2002a).
2. Assume a density at the inlet and calculate the velocity based on this assumption using Eq. (10).

If assumption one is chosen, and the velocity at the inlet is said to be sonic, the velocity follows from

$$v = \sqrt{\gamma RT} \ . \tag{12}$$

Neither of these two approaches are optimal and under certain circumstances the errors in the inlet conditions may be large.

The inlet conditions are applied to the model through ambient elements where the temperature and density are prescribed. In addition, velocities are prescribed to the nodes on the top surface of the ambient elements.

The base inlet parameters were chosen to be a constant mass flow rate of 0.75 kg/s. This mass flow rate gives a head form acceleration of approximately 2000 m/s^2, and a mean bag over-pressure of 10 kPa after 30 ms.

4.3 Venting holes

In order to achieve a softer impact between the occupant and the airbag in the standard in-position situations, airbags have venting holes on the back side of the bag. Gas can leak out through these hole and thereby reduce the pressure in the bag at impact.

Before the optimization started, it was investigated how the position of these holes could affect the maximum head form acceleration. The results showed that the position had no effect on the maximum acceleration, since the maximum acceleration occurs at the early stages of the inflation process when the dynamic effects are high, but the pressure is low. Thus, there is no flow out through the venting holes. This result was also confirmed in a study where the venting holes were removed. Therefore the vent hole position parameter was not included in the optimization process.

4.4 Formulation of the optimization problem

The optimization problem is written as

$$\begin{aligned} &\text{minimize}(\max a_{HF}) \\ &\text{subjected to} \\ &p_b(t = 0.03) > 20\,\text{kPa} \\ &0\,\text{kg/s} < q_n < 1.5\,\text{kg/s} \ , \end{aligned} \tag{13}$$

where a_{HF} is the acceleration of the head form, p_b is the mean over-pressure in the bag and $q_n, n = 1, 8$ are the design variables. The pressure constraint is enforced since the airbag must behave normally under in-position conditions. To analyze this correctly, we would need to run each simulation twice. One with the head form and one without. It was chosen, for efficiency reasons, that this constraint would be enforced when the head form was present.

The cost function a_{HF} is simply extracted by measuring the acceleration of the rigid body. The pressure constraint is more difficult to extract since the pressure is recorded at each integration point in every fluid element. This problem was solved by recording the pressure from five different elements, and taking the mean value of those pressures.

To solve this optimization problem the LS-OPT package, see Stander (1999), is used.

4.5
Results of the optimization

As this optimization problem has eight design variables and we are using linear response surfaces, 12 design points are chosen in each iteration, according to the recommendation from Redhe et al. (2002a). After 10 iterations had finished, convergence was not reached in the sense that both cost and constraint functions have reached stable values, and the decision to terminate the optimization was taken. At this point 140 simulations were made, which ends up at 2240 h of cpu time, roughly two months. This time was reduced by using a cluster of Linux computers, where 12 simulations can be run simultaneously, reducing the elapsed clock time to about 6 days.

The convergence of cost and constraint can be seen in Figs. 8 and 9. We note that in the last iteration the pressure constraint is slightly below the requested pressure of 20 kPa and perhaps the results from iteration 9 would be a more optimal solution. One or two more iterations would be needed to reach a fully converged solution. The history of the design variables is shown in Appendix A.

The computed results together with the surface approximation results from iteration 9 and 10 are shown in Table. 1.

Clearly the errors observed from iteration 9 is lower than the errors in iteration 10.

Figure 10 shows the optimized mass flow curve. The peak in mass flow rate at 1 ms (i.e. q_1) fills the bag until solid contact with the head form is established. Thereafter, the flow rate is decreased in order to reduce the resulting acceleration, and again increased to fulfill the pressure constraint.

We note that the head form acceleration has decreased from 2000 m/s^2 to 700 m/s^2, a reduction of 65% using the results from iteration 10. If instead the results from iteration 9 is used, the head form acceleration is reduced by 68% to 638 m/s^2. The acceleration for the initial and optimal designs are shown in Fig. 11. The optimal curve "smears out" the acceleration, whereas the initial design gives high acceleration values under a short period of time.

In Figs. 12–15 the inflation of the bag, using the optimal parameters, is shown. The plots show the free surface of the fluid inside the bag. Inlet velocity profiles are shown in Figs. 16–19. Three quarters of the fluid mesh and the airbag mesh have been blanked out and the velocity profiles are shown using the velocity vectors of the visible nodal points.

Figures 20 and 21 show the pressure distribution in the bag at $t = 5$ ms, which is the time where we have the highest head form accelerations. The pressure values listed are the highest pressures outside the proximity of the inflator.

5
Conclusions

This study shows that response surface optimization methods can successfully be applied together with coupled fluid-structure analysis for airbag inflation problems in order to reduce occupant injury. The results for this simplified system show that it can be possible to reduce the occupant injury with about 65% without compromising a safe design.

One must keep in mind that this problem is simplified compared to real world airbags and inflation processes, where e.g. a lid covers the airbag. This lid is opened as the airbag gets pressurized in its container and a tear seam is ripped open. We also do not account for such parameters as initial occupant velocity, initial occupant position or occupant weight.

If an optimization like this could include those parameters combined with a crash test dummy model, c.f. Fredriksson (1996), optimized mass flow curves for many hazardous situations would be found. Combined with advanced control systems, a drastic reduction of the number of airbag induced fatalities would be possible.

References

Anderson J (1982) Modern compressible flow, McGraw-Hill, New York

Belytschko T, Liu WK, Moran B (2000) Nonlinear Finite Elements for Continua and Structures, Wiley, Chichester

Fredriksson LA (1996) A Finite Element Data Base for Occupant Substitutes. Ph.D thesis no. 447, Div. of Solid Mech. Linköping University, Linköping

Hallquist JO (1998) LS-DYNA Theoretical Manual, Livermore Software Technology Corp, Livermore

Hughes TJR (1987) The Finite Element Method – Linear Static and Dynamic Finite Element Analysis, Prentice-Hall, Engelwood Cliffs

Kamiji K, Kawamura N (2001) Study of Airbag Interference with Out of Position Occupant by the Computer Simulation, 17th Int'l Conf. on Enhanced Safety of Vehicles, Amsterdam

Marklund P-O, Nilsson L (2001) Optimization of a car body component subjected to side impact. Structural and Multidiciplinary Optimization 21: 383–392

Marklund P-O, Nilsson L (2002a) Simulation of airbag inflation processes using a coupled fluid structure approach. Comput. Mech.

Marklund P-O, Nilsson L (2002b) A new fluid-structure coupling algorithm suitable for airbag inflation problems with permeable fabric. Comput. Mech.

Mestreau E, Löhner L (1996) Airbag Simulation using Fluid/Structure Coupling, 34th Aerospace Sciences Meeting & Exhibit, AIAA-96-0798, Reno

Myers RH, Montgomery DC (1995) Response Surface Methodology, Wiley, New York

National Highway Traffic Safety Administration (2001) Counts for Air Bag Related Fatalities and Seriously Injured Persons, Report NHTSA, Washington

Olovsson L (2000) On the Arbitrary Lagrangian–Eulerian Finite Element Method, Ph.D thesis no. 635, Div. of Solid Mech., Linköping University, Linköping

Phen RL, Dowdy MW, Ebbeler DH, Kim EH, Moore NR, VanZandt TR (1998) Advanced Air Bag Technology Assessment: Final Report, NASA – Jet Propulsion Laboratory, NHTSA, Washington

Redhe M, Forsberg J, Jansson T, Marklund PO, Nilsson L (2002) Using the response surface methodology and the D-optimality criterion in crashworthiness related problems – an analysis of the surface approximation error versus the number of function evaluations. Struct. Multidisciplinary Optim.

Redhe M, Jansson T, Nilsson L (2002) Using surrogate models and response surfaces in structural optimization – with application on crashworthiness design and sheet metal forming. Struct. Multidisciplinary Optim.

Roux WJ, Stander N, Haftka RT (1998) Response surface approximations for structural optimization. Int. J. Numer. Meth. Eng. 42: 517–534

Stander N (1999) LS-OPT Users Manual, Livermore Software Technology Corp., Livermore

Stander N (2001) The successive response surface method applied to sheet–metal forming. First MIT Conference on Computational Fluid and Solid Mechanics, Boston

Ullrich P, Trameçon A, Kuhnert J (2000) Advanced air bag fluid structure coupled simulations applied to out of position simulations. Europam Conference, Nantes

Zhu Y, Wickramasinghe K, Francis N (1999) Fluid structure interaction modeling of airbag deployment using PAM-FLOW/PAM-CRASH coupling. Ameripam Conference

Appendix A: Design variable iteration history

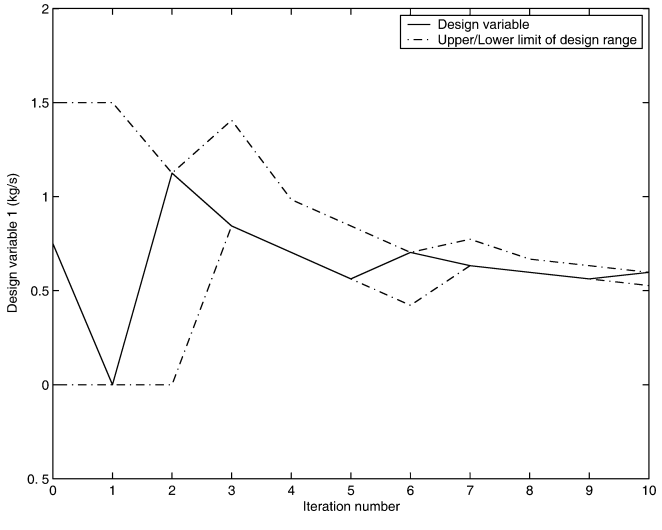

Fig. 22. Iteration history for design variable 1

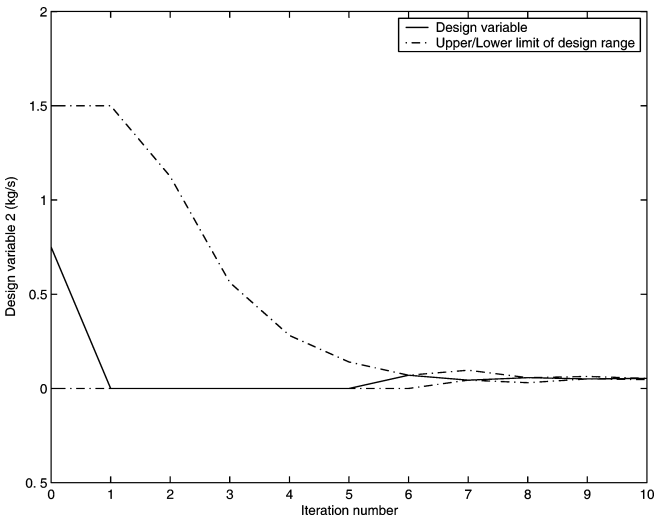

Fig. 23. Iteration history for design variable 2

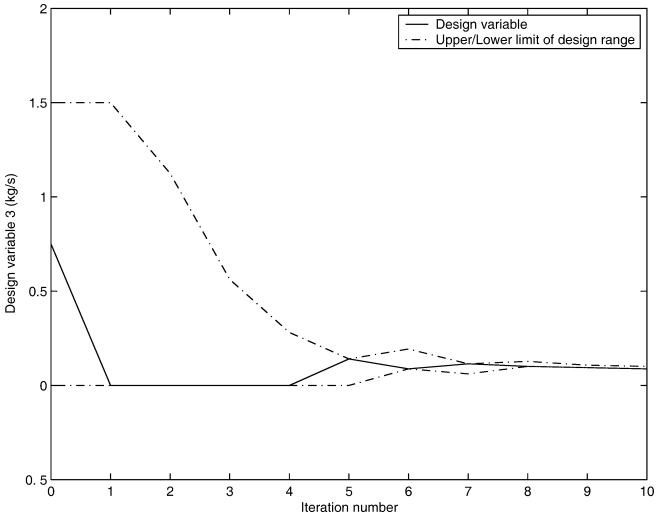

Fig. 24. Iteration history for design variable 3

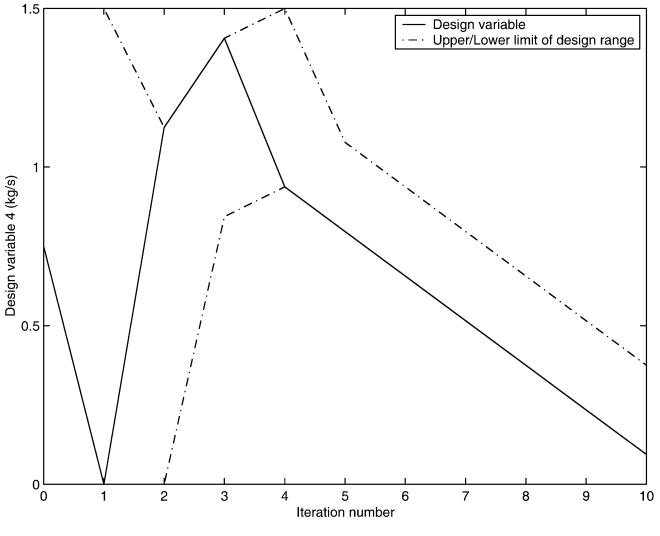

Fig. 25. Iteration history for design variable 4

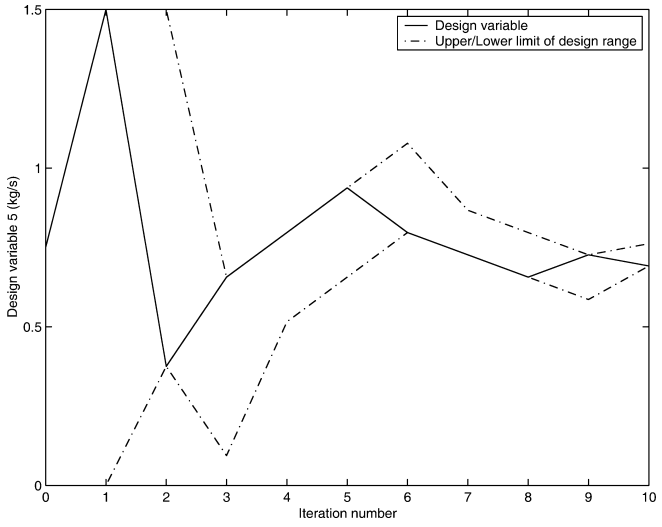

Fig. 26. Iteration history for design variable 5

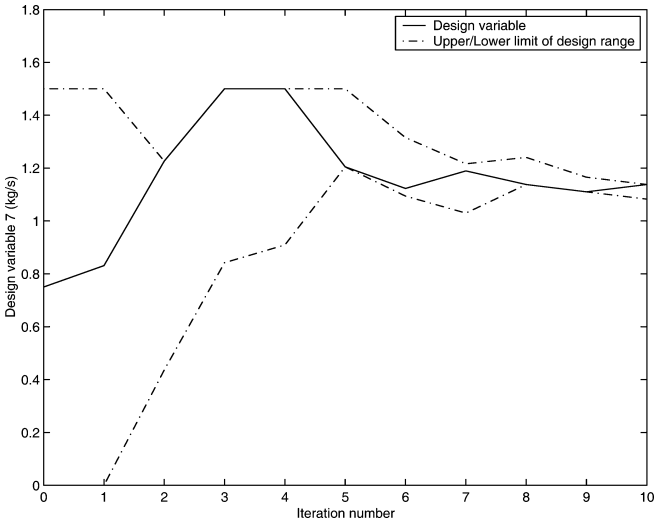

Fig. 28. Iteration history for design variable 7

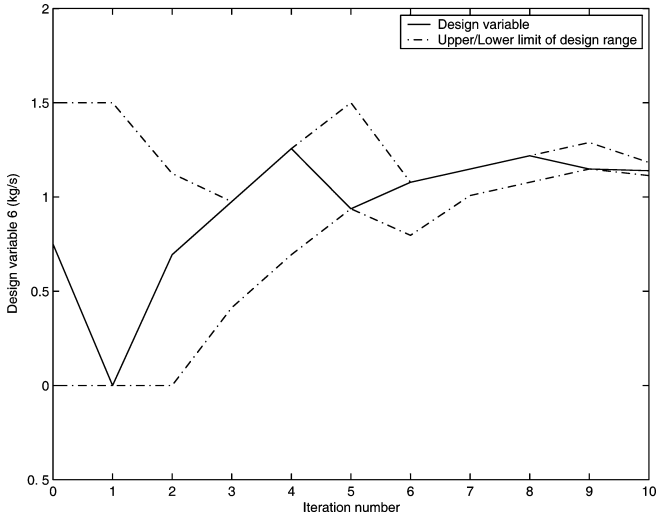

Fig. 27. Iteration history for design variable 6

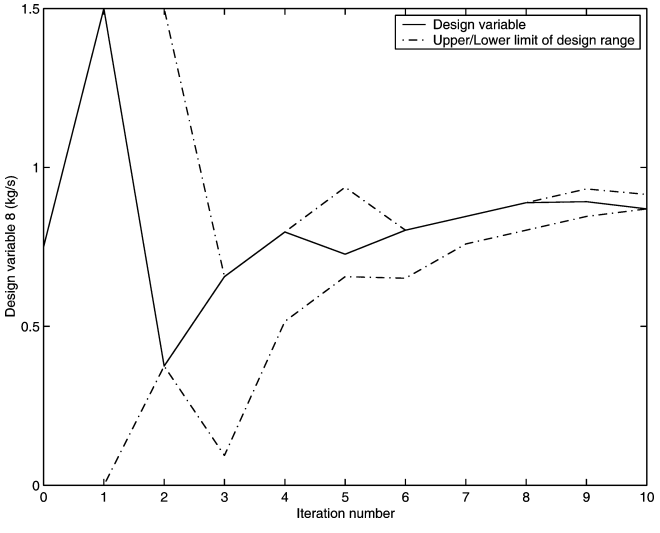

Fig. 29. Iteration history for design variable 8